

## Oxygen electrodes for rechargeable alkaline fuel cells. III

L. Swette\*, N. Kackley and S. A. McCatty

Giner, Inc., Waltham, MA 02254-9147 (U.S.A.)

### Abstract

The investigation and development of electrocatalysts and supports for the positive electrode of moderate-temperature single-unit rechargeable alkaline fuel cells is described with focus on chemical and electrochemical stability and O<sub>2</sub> reduction/evolution activity.

### Introduction

The work presented here represents an update of the continuing investigation of candidate materials for moderate temperature single-unit rechargeable alkaline fuel cells, some of which have been described previously [1-3]. The focus is on new and previously studied materials which have undergone testing to either qualify them for further investigation and potential development or disqualify them for use in the rechargeable alkaline fuel cell application.

Viable candidate materials must meet the following requirements: (i) good electrical conductivity (a more demanding requirement for supports than electrocatalysts); (ii) high resistance to chemical corrosion and electrochemical oxidation and/or reduction; (iii) electrocatalysts, in addition, must exhibit high bifunctional electrocatalytic activity (O<sub>2</sub> evolution and reduction). Advanced development requires that the materials be prepared in high-surface-area forms, and may also entail integration of various candidate materials, e.g. one or two electrocatalysts unsupported or distributed on a stable conductive support.

Candidate support materials have been drawn from transition metal carbides, nitrides and oxides which have high electrical conductivity. Some candidate support materials exhibit catalytic activity for O<sub>2</sub> evolution and/or reduction. These materials, generally noble metal-containing oxides, are termed catalytic supports. Candidate catalyst materials have been selected largely from metal oxides of the form ABO<sub>x</sub> (where A = Pb, Mn, Ti, Ni, Co, Zr, Na, and B = Pt, Ir, Rh, Ru). Some of these have been investigated and/or developed for one function only, either O<sub>2</sub> reduction or O<sub>2</sub> evolution. The electrical conductivity requirement for catalysts may be lower, especially if integrated with a higher conductivity support. For initial evaluation, materials

---

\*Author to whom correspondence should be addressed.

have been purchased when available; subsequently, in-house preparations have been attempted, to affect surface area and composition, when necessary.

Candidate materials of acceptable conductivity are typically subjected to corrosion testing in three steps. Preliminary corrosion testing consists of exposure to 30% KOH at 80 °C under oxygen for about 5 days. Materials that survive chemical testing are examined for electrochemical corrosion activity; the material is held at 1.4 V versus reversible hydrogen electrode (RHE) in 30% KOH at 80 °C for 15 to 20 h. An acceptable anodic current is on the order of a few  $\mu\text{A}/\text{mg}$  of material. For more stringent corrosion testing, and for further evaluation of electrocatalysts (which generally show significant  $\text{O}_2$  evolution at 1.4 V), samples are held at 1.6 V for about 100 h and at 0.6 V for about 16 h. The surviving materials are then physically and chemically analyzed for signs of degradation (visual examination, electron microscopy, X-ray diffraction).

To evaluate the bifunctional oxygen activity of candidate catalysts, Teflon-bonded electrodes are fabricated and tested in a floating electrode configuration [4]. Many of the experimental materials being studied have required development of a customized electrode fabrication procedure. For preliminary testing, catalysts of interest should show  $<500$  mV polarization (from 1.2 V) in either mode at  $200 \text{ mA}/\text{cm}^2$ . In advanced development, the goal is to reduce the polarization to about 300–350 mV.

## Materials investigated

Materials were originally assigned to the categories of support or electrocatalyst based on reported or anticipated performance. Some of the metal ratios shown are the targeted synthesis compositions only.

### *Candidate supports*

$\text{LiNiO}_x$ ,  $\text{TiN}$ ,  $\text{ZrC}$ ,  $\text{ZrN}$ .

### *Candidate catalytic supports*

$\text{LaNiO}_3$ ,  $\text{PbPdO}_2$ ,  $\text{CoIrO}_3$ ,  $\text{NiIrO}_3$ ,  $\text{RhO}_2$ ,  $\text{IrO}_2$ .

### *Candidate electrocatalysts*

$\text{Na}_x\text{Pt}_3\text{O}_4$ ,  $\text{Pb}_2(\text{Ir}_{2-x}\text{Pb}_x)\text{O}_{7-y}$ , Rh black, Pt black,  $\text{IrMnO}_x$ ,  $\text{IrNiO}_x$ ,  $\text{IrNi}_3\text{O}_x$ ,  $\text{IrTi}_{1.25}\text{O}_x$ ,  $\text{PtTi}_{1.5}\text{O}_x$ ,  $\text{PtTi}_2\text{O}_x$ ,  $\text{PtZr}_2\text{O}_x$ ,  $\text{RuTiO}_x$ ,  $\text{RuMn}_2\text{O}_x$ ,  $\text{RuMn}_3\text{O}_x$ ,  $(\text{RuIr})\text{Mn}_2\text{O}_x$ .

### *Reference materials*

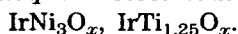
$\text{O}_2$  reduction: 10% Pt/Au (Johnson-Matthey,  $11 \text{ m}^2/\text{g}$ ).

$\text{O}_2$  evolution: Pt black (Englehard,  $25 \text{ m}^2/\text{g}$ ).

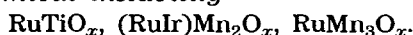
Several candidate materials have been eliminated from further consideration for various reasons, as shown below. Some of the noble-metal/transition-metal mixed oxide preparations resulted in two-phase materials

consisting of a noble metal or noble metal oxide (e.g. Pt, RuO<sub>2</sub> or IrO<sub>2</sub>) and a transition metal oxide (e.g. TiO<sub>2</sub>, ZrO<sub>2</sub>, Mn<sub>2</sub>O<sub>3</sub>). These materials may show adequate conductivity and even some catalytic activity due to the noble metal or noble metal oxide component, but they were not investigated further.

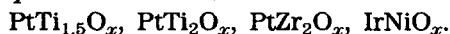
*Inadequate electrical conductivity*



*Chemical instability*



*Two-phase mixed oxide*



### Sources of candidate materials

Candidate materials for both catalysts and supports were purchased, if commercially available in powder form, as the most efficient approach for preliminary evaluation (electrical conductivity, chemical and electrochemical stability). Such materials offer the advantage of an economical purchase of a material of known purity in a quantity (5–25 g) sufficient for preliminary qualification, and particularly for disqualification. The disadvantage is that most of the commercially available materials have surface areas in the range from low (< 10 m<sup>2</sup>/g) to very low (< 1 m<sup>2</sup>/g). Consequently, most commercial materials that survive preliminary screening must be prepared in a higher surface area form, in-house or by a custom fabricator, for effective evaluation as potential catalysts and/or supports.

In many cases, especially for candidate catalysts, commercial materials were not available. Preparation methods described in the literature, either specific for the material or as a general model, were used when deemed appropriate to the material requirements in terms of yielding an electrically conductive, high-surface-area powder. IrO<sub>2</sub> and RhO<sub>2</sub> were prepared by the Adams method [5]. Na<sub>x</sub>Pt<sub>3</sub>O<sub>4</sub> was prepared typically by firing Na<sub>2</sub>CO<sub>3</sub> and PtO<sub>2</sub> at > 600 °C [1–3, 6, 7]. Synthesis of nickel–iridium oxide was attempted by the Adams method of fusion of the metal chlorides in sodium nitrate [5], but this yielded a two-phase product. As an alternative, NiIrO<sub>3</sub> and CoIrO<sub>3</sub> were prepared following the method of Chamberland and Silverman [8]; this consists of co-precipitation of the hydroxides and firing at 350 °C. X-ray diffraction analysis has not been carried out because prior work [8] has indicated that, although the materials have the elemental compositions of ilmenites, they are not crystalline. Both materials had good surface area and conductivity, but the CoIrO<sub>3</sub> material showed higher values in both measurements. No chemical or electrochemical stability tests have been completed on these two materials to date.

## Characterization of candidate support materials

Candidate material preparations are typically analyzed by X-ray diffraction (XRD) for chemical characterization. The objective of preparing fine powder materials, however, is generally in conflict with obtaining sharp XRD patterns (because of the line-broadening characteristic of high-surface-area powders); thus the quality of these results is sometimes compromised. Firing materials for a longer time or at a higher temperature usually increases the crystallinity and improves XRD results, but at the expense of decreased surface and some uncertainty about the composition of the original higher surface area material. In some instances, materials of interest have been re-analyzed by XRD and/or scanning electron microscopy (SEM) after extended corrosion testing to check for changes in composition, reaction products and changes in morphology. SEM has also been used occasionally to observe the particle size range of powders.

A summary of the measured physical characteristics of candidate materials is presented in Table 1. The electrical conductivity of candidate materials is estimated by compressing a small volume (e.g. 0.5–1 cm<sup>3</sup>) of the powder at about 12 000 psi between metal pistons within an insulating cylinder. The resistance is determined by measuring the voltage drop across the powder under the flow of sufficient current to generate easily measured current and voltage signals. The more accurate 4-point method of measuring resistance has not been used because of the larger sample volume requirement. Surface areas of candidate materials are determined by the BET nitrogen adsorption method using a Micromeritics Flowsorb II 2300 instrument.

## Stability testing

A preliminary assessment of the *chemical stability* of the candidate support materials is made by exposing the as-prepared powder to 30% KOH at 80 °C under an oxygen atmosphere for about 5 days, as described in previous publications [1–3]. This test is useful for eliminating the more unstable candidate materials.

For an initial assessment of the *electrochemical stability* of candidate support materials and catalysts, a wettable electrode composition is prepared on gold mesh and the steady-state anodic current is measured in the range of 1.0 to 1.4 V versus RHE in 30% KOH at 80 °C. If the anodic current observed, after initiation of potentiostatic control at 1.4 V, drops to the microamp range, the system is allowed to equilibrate overnight; the steady-state anodic current is then recorded. In a second stage of testing, candidate materials are subjected to higher potentials (1.6 V) representative of oxygen evolution conditions for about 100 h, and lower potentials (0.6 V) representative of oxygen reduction conditions for about 16 h. The latter is intended to place electrochemical stress on the materials used in the oxide form. The current values measured are combined with other observations such as weight

TABLE 1  
Physical characterization of candidate materials<sup>a</sup>

Material	Source [Reference]	Surface area (m <sup>2</sup> /g)	Electrical conductivity (Ω cm <sup>-1</sup> )
Pt	Engelhard	25	N/M
Rh	Johnson Matthey	39	N/M
Na <sub>0.7</sub> Pt <sub>3</sub> O <sub>4</sub>	Giner, Inc. no. 1 [1-3, 6, 7]	21	50
	Giner, Inc. no. 2 [1-3, 6, 7]	17	56
Pb <sub>2</sub> (Ir <sub>1.33</sub> Pb <sub>0.67</sub> )O <sub>7-y</sub>	Giner, Inc. no. 1 (400 °C) [10]	24	40
Pb <sub>2</sub> (Ir <sub>2-x</sub> Pb <sub>x</sub> )O <sub>7-y</sub>	Giner, Inc. no. 3 [5]	95	64
RuMn <sub>2</sub> O <sub>x</sub>	Giner, Inc. no. 1 [5]	62	2.9
IrMn <sub>2</sub> O <sub>x</sub>	Giner, Inc. no. 1 [5]	45	12
IrO <sub>x</sub>	Giner, Inc. no. 1 [5]	160	70
	Giner, Inc. no. 2 [5]	198	33
RhO <sub>2</sub>	Giner, Inc. no. 1 [5]	187	14
ZrC (2% Hf)	Aesar	1	125
ZrC (Hf free)	Alfa Prod.	0.6	125
ZrC + Zr (SPHTS)	Giner, Inc. [9]	38	34
TiN	Alfa Prod.	N/M	390
	Giner, Inc.	2.3	440
	Univ. of California no. 2	56	0.34
	Univ. of California no. 3	38	N/M
	Univ. of California no. 5	21	14
	U. of C. no. 5 (950 °C, 5% H <sub>2</sub> /N <sub>2</sub> )	20	> 700
NiIrO <sub>3</sub>	Giner, Inc. [8]	47	16
CoIrO <sub>3</sub>	Giner, Inc. [8]	57	47

<sup>a</sup>Code: N/M, not measured.

loss or gain, color changes, changes in conductivity, microscopic examination (SEM, TEM) and analysis (EDAX, XRD, etc.) to assess the stability of the material.

Observations on chemical stability are summarized in Table 2. Electrochemical stability measurements are recorded in Tables 3 and 4.

*LaNiO<sub>3</sub>*, *LiNiO<sub>x</sub>* and *ZrN* are potentially promising support materials, as described previously [1-3], but have not been investigated further.

The following observations were made on candidate materials tested.

### *TiN*

In previous work, the coarse commercial powder (< 40 μm) and the low-surface-area Giner, Inc. preparation (1 μm, 2.3 m<sup>2</sup>/g) appeared to be quite stable at oxygen evolution potentials [2, 3]. Post-test XRD analysis indicated a strong TiN pattern ( $a = 4.240 \text{ \AA}$ ), no TiO<sub>2</sub>, and a few lines possibly due to a silicate, phosphate or carbonate. The higher-surface-area material,

TABLE 2

Results of stability tests of selected candidate materials<sup>a</sup>

Material	Source [Reference]	Weight change (%)	Observations
Na <sub>0.7</sub> Pt <sub>3</sub> O <sub>4</sub>	Giner, Inc. no. 1 [1-3, 6, 7]	N/M	NVR
	Giner, Inc. no. 2 [1-3, 6, 7]	N/M	NVR
Pb <sub>2</sub> (Ir <sub>1.33</sub> Pb <sub>0.67</sub> )O <sub>7-y</sub>	Giner, Inc. no. 1 (400 °C) [10]	N/M	NVR
	Pb <sub>2</sub> (Ir <sub>2-x</sub> Pb <sub>x</sub> )O <sub>7-y</sub>	Giner, Inc. no. 3 [5]	-20
RuMn <sub>2</sub> O <sub>x</sub>	Giner, Inc. no. 1 [5]	-14	SR-C
	Giner, Inc. no. 1 KOH leached	-13	SR-C
	Giner, Inc. no. 1 650 °C, O <sub>2</sub>	-15	SR-C
IrMn <sub>2</sub> O <sub>x</sub>	Giner, Inc. no. 1 [5]	-9	NVR
IrO <sub>x</sub>	Giner, Inc. no. 1 [5]	-39	NVR
RhO <sub>2</sub>	Giner, Inc. [5]	0	NVR
ZrC (2% Hf)	Aesar	N/M	SR-G
ZrC (Hf free)	Alfa Prod.	-16	SR
TiN	Alfa	N/M	NVR
	Giner, Inc.	N/M	NVR
	Univ. of California no. 2	N/M	SR-C
	U. of C. no. 5 (950 °C, 5% H <sub>2</sub> /N <sub>2</sub> )	-2	NVR

<sup>a</sup>Codes: NVR, no visible reaction; SR, slight reaction (C = color, G = gas); N/M, not measured.

TiN<sub>x</sub>, ( $x = 0.72$  to  $0.86$ )\* similarly appeared relatively stable in the chemical test and anodically up to 1.4 V. However, dissolution occurred when the electrode was held at 1.6 V. A gold-catalyzed TiN electrode was also found to be very reactive. After electrochemical testing, the surface of the electrode had degraded to a refractory non-conductive material. Post-test XRD analysis showed a strong second phase, possibly potassium titanate. Tracking of electrical conductivity through electrode processing in air revealed that the material increased in resistivity by about a factor of 1000 at 325 °C, indicating oxidation. Sintering under 5% H<sub>2</sub>/N<sub>2</sub> preserved the conductivity, but did not improve stability [2].

A stoichiometric form of TiN may prove to be suitable as a support for O<sub>2</sub> reduction catalysts, but it seems unlikely that it will be a viable candidate support for O<sub>2</sub> evolution catalysts.

### ZrC

As described previously, a commercially available, coarse ( $< 40 \mu\text{m}$ ), low-surface-area powder with about 2% Hf impurity was evaluated [2, 3]. Gas generation was noted during the initial period of the chemical stability test, but this was attributed to dissolution of the Hf impurity (weight change measurements were not successful). Very low anodic currents were measured

\*TiN<sub>x</sub> prepared by Dr J. Michaels, Dept. of Chem. Eng., University of California at Berkeley.

TABLE 3

Electrochemical stability measurements on selected candidate materials

Material	Source [Reference]	Anodic current ( $\mu\text{A}/\text{mg}$ ) at 1.0–1.4 V (vs. RHE)				
		1.0	1.1	1.2	1.3	1.4
$\text{Na}_{0.7}\text{Pt}_3\text{O}_4$	Giner, Inc. no. 1 [1–3, 6, 7]	1.5	1.0	1.3	2.3	800
$\text{Pb}_2(\text{Ir}_{1.33}\text{Pb}_{0.67})\text{O}_{7-y}$	Giner, Inc. no. 1 (400 °C) [10]	23		32	50	
	Giner, Inc. no. 2 (500 °C) [10]			0.4	2.0	6.0
$\text{Pb}_2(\text{Ir}_{1-x}\text{Pb}_x)\text{O}_{7-y}$	Giner, Inc. no. 3 [5]	3.0	4.0	4.0	4.0	7.0
$\text{IrMn}_2\text{O}_x$	Giner, Inc. no. 1 [5]	1.0	1.0	2.0	5.0	400
$\text{IrO}_x$	Giner, Inc. no. 1 [5]	1.0	1.0	3.0	8.0	684
$\text{RhO}_2$	Giner, Inc. [5]	1.3	4.0	4.0	25	2100
ZrC (2% Hf)	Aesar	0.5	1.1	1.2	0.7	0.7
ZrC (Hf free)	Alfa	0.5	0.9	0.9	0.7	0.4
TiN	Alfa	0.2	0.2	0.2	0.2	0.2
	Giner, Inc.	0.4	0.4	0.6	0.5	0.6
	Univ. of California no. 2	1.0	2.0	2.0	1.0	3.5
	Univ. of California no. 3	0.4	0.9	1.3	0.5	1.5
	Univ. of California no. 5	1.3	1.3	1.2	0.5	0.2
TiN (air-sintered elect.)	U. of C. no. 5 (950 °C, 5% $\text{H}_2/\text{N}_2$ )	0.3	1.4	1.2	0.7	0.6
TiN (5% $\text{H}_2/\text{N}_2$ sinter)	U. of C. no. 5 (950 °C, 5% $\text{H}_2/\text{N}_2$ )	5.0	4.0	2.0	0.7	0.2

at 1.4 V, although in testing at 1.6 V versus RHE from 50 to 100 h, there was a visible loss of material, as well as a measurable weight loss (e.g. ~40%). This may have been due to physical shedding during oxygen evolution, as there was no other evidence of reaction.

A 'Hf-free' ZrC with similar conductivity, surface area and particle size, obtained from another vendor, was also investigated [2]. In chemical testing, no gassing or color changes were observed, but there was a weight loss of about 16% and a small amount of white flocculent precipitate. The electrical conductivity was *higher* after chemical stability testing (700 versus 125  $\Omega\text{ cm}^{-1}$ ). In electrochemical stability testing, the anodic currents measured at 1.4 V were low, 0.5 to 1.0  $\mu\text{A}/\text{mg}$ . The electrode was tested at 1.6 V versus RHE for approximately 81 h. There was a visible thinning of the electrode and a weight loss of 36%, similar to that seen in tests of Hf-containing material. X-ray analysis of the post-test electrode showed broad lines for a ZrC phase, plus a strong secondary phase which could not be positively identified, but may be a Teflon or carbonaceous species.

Preparation of high-surface-area ZrC by self-propagating high-temperature synthesis (SPHTS) was investigated. High-surface-area carbon and zirconium metal powder were combined and ignited with a resistance coil following the method of Mullins and Riley [9]. The SPHTS was partially

TABLE 4

Electrochemical stress tests on selected candidate materials

Material	Source [Reference]	Stress test		Observations (weight change)
		hours at 1.6 V	0.6 V	
$\text{Na}_{0.7}\text{Pt}_3\text{O}_4$	Giner, Inc. no. 1 [1-3, 6, 7]	120	70	no significant deterioration
$\text{Pb}_2(\text{Ir}_{1.33}\text{Pb}_{0.67})\text{O}_{7-y}$	Giner, Inc. no. 1 (400 °C) [10]		112	cracking, shrinkage
	Giner, Inc. no. 2 (500 °C) [10]	24	72	delamination at 0.6 V
$\text{Pb}_2(\text{Ir}_{2-x}\text{Pb}_x)\text{O}_{7-y}$	Giner, Inc. no. 3 [5]	108	21	slight reaction, gray particulate (-17%)
$\text{IrMn}_2\text{O}_x$	Giner, Inc. no. 1 [5]	102	17	color in solution (-17%)
$\text{IrO}_x$	Giner, Inc. no. 1 [5]	83	18	no significant deterioration (-5%)
$\text{RhO}_2$	Giner, Inc. [5]	87	18	no significant deterioration
ZrC (2% Hf)	Aesar	48	17	material loss (-38%)
ZrC (Hf free)	Alfa	81	18	material loss (-36%)
TiN	Giner, Inc.	105		surface color change (0%)
	Univ. of California no. 3	46		partially dissolved
	Univ. of California no. 5	3		XRD analysis TiN + $\text{K}_2\text{TiO}_3$ ? (+5%)

successful, but X-ray diffraction analysis indicated that the product contained about 50% unreacted Zr. No further investigation of ZrC is planned.

### $\text{PbPdO}_2$

A preparation of this compound by the Adams method, reported previously [2, 3], had a very low surface area, but appeared to be quite stable in electrochemical testing. Attempts to prepare a higher-surface-area material have been unsuccessful to date.

### $\text{Na}_x\text{Pt}_3\text{O}_4$

Some initial preparations of this compound, described in previous publications [1-3], were determined by XRD to be single-phase  $\text{Na}_x\text{Pt}_3\text{O}_4$  with apparent  $x$  values of 0.7-0.8. In a 17-day electrochemical stability test, this material showed no evidence of degradation. In a more demanding test, two  $\text{Na}_x\text{Pt}_3\text{O}_4$  electrodes were cycled between oxygen reduction and evolution for about 90 h (45 one-hour cycles; see Fig. 2 and description in discussion of oxygen performance). At the conclusion of this test, both electrodes were subjected to XRD analysis (the final state of each electrode, reduction or evolution, was not recorded). Both catalysts exhibited the crystallographic pattern for  $\text{Na}_x\text{Pt}_3\text{O}_4$ , but the value of  $x$  for the catalyst from one electrode may have been reduced slightly. X-ray diffraction peak broadening allows only very approximate determination of the unit cell parameter needed to establish  $x$  values ( $\pm 0.2$ ), thus we have not been able to establish a correlation



between this parameter and physical characteristics and performance. For several more recent preparations, we have performed elemental analysis by inductively coupled plasma spectroscopy (ICP) to determine the sodium content. These measurements indicate a much lower value for  $x$  ( $\sim 0.5$ ) than estimated from XRD data. A preliminary conclusion is that the  $\text{Na}_x\text{Pt}_3\text{O}_4$  compositions with higher  $x$  values are more conductive and may also be more catalytically active.

### $\text{Pb}_2(\text{Ir}_{2-x}\text{Pb}_x)\text{O}_{7-y}$

In prior work [1], material prepared by a low-temperature precipitation method, based on a procedure described by Horowitz *et al.* [10], was found to be unstable in 30% KOH at 80 °C and showed substantial physical changes at 1.6 V. Refiring at 500 °C improved crystallinity and decreased reactivity below 1.4 V. The test electrode survived 24 h at 1.6 V, but delaminated from the current collector at 0.6 V [2, 3]. Another method to prepare  $\text{Pb}_2(\text{Ir}_{2-x}\text{Pb}_x)\text{O}_{7-y}$ , by fusion of the respective salts in sodium nitrate [5], was investigated. The product had good surface area (95  $\text{m}^2/\text{g}$ ) and conductivity (64  $\Omega\text{ cm}^{-1}$ ). The as-prepared material could not be analyzed due to lack of crystallinity. After heat treatment in oxygen at 750 °C to increase particle size and crystallinity, X-ray diffraction analysis showed a 50/50 mixture of  $\text{IrO}_2$  and the Pb-substituted pyrochlore. The effect of the heat treatment on the original composition is unknown. The lattice parameter of the pyrochlore was 10.316 Å, which leads to an approximate formula of  $\text{Pb}_2(\text{Ir}_{1.9}\text{Pb}_{0.1})\text{O}_{7-y}$ . In chemical stability tests, a 20% weight loss was measured. This material showed some catalytic activity, as described in the next section.

### $\text{RhO}_2$

This material was also prepared by fusion of a Rh salt in sodium nitrate [5]. The product showed excellent surface area (187  $\text{m}^2/\text{g}$ ) and conductivity (14  $\Omega\text{ cm}^{-1}$ ). X-ray diffraction and thermogravimetric analyses showed the material to be  $\text{RhO}_2 \cdot (0.48)\text{H}_2\text{O}$ . In chemical stability tests, no weight loss was seen. Electrochemical stability testing also showed no significant weight loss, after 87 h at 1.6 V and 18 h at 0.6 V. The current densities measured were relatively high, at 1.3 to 1.6 V, due to the catalytic activity of the material. As described in the next section,  $\text{RhO}_2$  shows potential as a catalyst and/or catalytic support material.

### $\text{IrO}_2$

The sodium nitrate fusion method [5] was also used to prepare two different batches of high-surface-area  $\text{IrO}_2$  (160 to 198  $\text{m}^2/\text{g}$ ) with excellent conductivity (33 to 70  $\Omega\text{ cm}^{-1}$ ). X-ray analysis confirmed that the material (batch no. 2) was single-phase  $\text{IrO}_2$ . Scanning electron microscopy showed a mix of thin platelets of several microns in width, as well as agglomerations of submicron-sized particles. In the chemical stability test, the batch no.1 material showed no visible change, but exhibited a 39% weight loss. This result is not consistent with the electrochemical test and may be a result

of experimental error. In the electrochemical stability test, the  $\text{IrO}_2$  electrode showed 1 to 8  $\mu\text{A}/\text{mg}$  at 1.0 to 1.3 V. There is significant oxygen evolution activity above 1.3 V. After a total test time of 83 h at 1.6 V and 18 h at 0.6 V in 30% KOH at 80 °C, the electrode showed no significant deterioration and a weight loss of only 5%. This material shows significant promise, both as a catalyst and as a catalytic support and has been combined with Pt to form a bifunctional electrode as described in the next section.

#### *IrMn<sub>2</sub>O<sub>x</sub>*

This material had higher conductivity ( $12 \Omega \text{ cm}^{-1}$ ) but slightly lower surface area than  $\text{RuMn}_2\text{O}_x$ . In preliminary chemical stability tests, it appeared more stable and did not cause a color change in the KOH solution. However, a yellow coloration was noted during the electrochemical stress test, along with a 17% weight loss from the test electrode. The  $\text{IrMn}_2\text{O}_x$  displayed considerable catalytic activity, as described below, and may merit further investigation. This material could not be analyzed in the as-prepared form because of its high surface area (small particle size) and possible lack of crystallinity. A heat-treated sample (900 °C in  $\text{O}_2$ ) showed a broad-line rutile phase in X-ray diffraction analysis. An approximate composition of  $\text{Ir}_{1-x}\text{Mn}_x\text{O}_2$ , where  $x$  was 0.05–0.10, was determined. However, the effect of the heat treatment on the chemical composition is unclear.

#### *RuMn<sub>2</sub>O<sub>x</sub>*

This material showed evidence of instability in chemical and electrochemical stability tests (weight loss and color change of the KOH). After leaching in KOH in order to remove any soluble component, the material still showed a 13% weight loss on exposure to 80 °C KOH and produced coloration of the KOH solution. Another sample of the as-prepared  $\text{RuMn}_2\text{O}_x$  was heat treated at 650 °C in oxygen. This treatment caused a large loss in surface area from 62 to 12  $\text{m}^2/\text{g}$ , and increased the conductivity slightly from 2.9 to 5.6  $\Omega \text{ cm}^{-1}$ . As before, the chemical stability was not improved (15% weight loss and coloration of the KOH solution were observed). The leached and heat-treated samples were not subjected to electrochemical stress testing.

### Oxygen electrode performance testing

Oxygen electrode performance testing was performed in a floating electrode cell [4] in 30% KOH at 80 °C using a 1 cm × 1 cm electrode sample, as described in earlier publications [1–3]. The reference materials for  $\text{O}_2$  reduction and  $\text{O}_2$  evolution were 10% Pt/Au and Pt black, respectively. All candidate catalysts were compared to these reference materials as well as to each other.

The testing sequence is usually an oxygen reduction polarization test followed by an oxygen evolution polarization test, applying small potential

steps sufficient to yield a few data points in each log-decade of current density from 1 to 1000 mA/cm<sup>2</sup>. The potentials are controlled, and compensated for IR loss, with a Princeton Applied Research model 173 potentiostat. Collecting oxygen evolution data entails frequent interruptions to remove trapped gas bubbles. After an oxygen evolution test, electrodes that have not been optimized for bifunctional operation are sometimes too flooded to rerun an oxygen reduction test. Development of an electrode structure adequate for bifunctional operation with these candidate electrocatalysts is an independent research task. Some electrodes have been prepared using processing methods designed for optimization of bifunctional performance. Results on O<sub>2</sub> reduction and O<sub>2</sub> evolution tests on these electrodes are very promising, as described at the end of this section.

### *NiIrO<sub>3</sub> and CoIrO<sub>3</sub>*

Both of these candidate support materials showed some oxygen redox activity in preliminary testing, as shown in Fig. 1. The CoIrO<sub>3</sub> was poor in O<sub>2</sub> reduction, but is promising for O<sub>2</sub> evolution. After stability testing, further electrode development will be pursued if warranted.

### *IrMn<sub>2</sub>O<sub>x</sub>*

This material displayed excellent O<sub>2</sub> reduction and O<sub>2</sub> evolution performance, as shown in Fig. 1, but this level of performance proved difficult to reproduce on subsequent tests. As discussed above, this material shows signs of instability in anodic corrosion testing and requires further development, but it remains an interesting candidate for bifunctional oxygen catalysis.

### *IrO<sub>2</sub>*

This material was tested for comparison to the other iridium-based catalysts prepared. It can be seen that the oxygen evolution performance

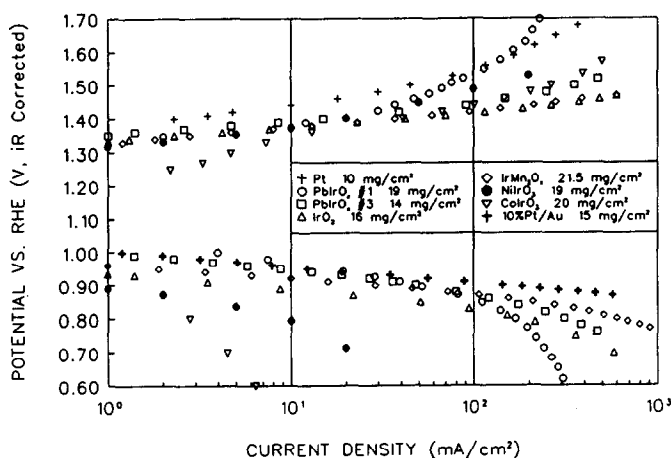


Fig. 1. O<sub>2</sub> reduction/evolution performance of Ir-containing electrodes, 30% KOH, 80 °C.

of  $\text{IrMn}_2\text{O}_x$  is similar to  $\text{IrO}_2$ , but the oxygen reduction performance of  $\text{IrMn}_2\text{O}_x$  is better. The latter effect may be due to electrode structural differences for the two materials.

### $\text{Pb}_2(\text{Ir}_{2-x}\text{Pb}_x)\text{O}_{7-y}$

As shown in Fig. 1, this Adams fusion preparation (no. 3, which turned out to contain two phases,  $\text{Pb}_2(\text{Ir}_{1-x}\text{Pb}_x)\text{O}_{7-y}$  and  $\text{IrO}_2$ ) showed better  $\text{O}_2$  reduction performance than  $\text{IrO}_2$  alone, but was not as good as the  $\text{IrMn}_2\text{O}_x$  material. For  $\text{O}_2$  evolution, it was slightly poorer than  $\text{IrO}_2$  alone or  $\text{IrMn}_2\text{O}_x$ . At low current densities, this material showed performance similar to single-phase  $\text{Pb}_2(\text{Ir}_{1.33}\text{Pb}_{0.67})\text{O}_{7-y}$  prepared previously (no. 1) by the Horowitz method [10]. At higher current densities, it showed much improved performance (e.g. above about  $50 \text{ mA/cm}^2$  in  $\text{O}_2$  evolution mode and above about  $200 \text{ mA/cm}^2$  in  $\text{O}_2$  reduction mode). Some of these differences in performance may be due to differences in the electrode structure.

### $\text{Na}_x\text{Pt}_3\text{O}_4$

The  $\text{Na}_x\text{Pt}_3\text{O}_4$  catalyst [1-3, 6, 7] was evaluated in an  $\text{O}_2/\text{O}_2$  cell under cyclic  $\text{O}_2$  evolution/reduction conditions. Two  $\text{Na}_x\text{Pt}_3\text{O}_4$  electrodes were separated by a matrix material soaked in 30% KOH. The full cell was operated under a positive pressure oxygen atmosphere (50 psi) at  $80^\circ\text{C}$ . The cell voltage was measured at current densities of 50, 100 and  $200 \text{ mA/cm}^2$ .

One electrode underwent 30 min on  $\text{O}_2$  reduction, 5 min on open circuit, then 30 min on  $\text{O}_2$  evolution, while the other electrode was undergoing the opposite cycle. The measured voltage represents the difference between the electrode potentials, which may be positive or negative, depending on which electrode is at the  $\text{O}_2$  evolution potential. Figure 2 shows the cell potential on progressive cycling at each current density. The cell polarization was

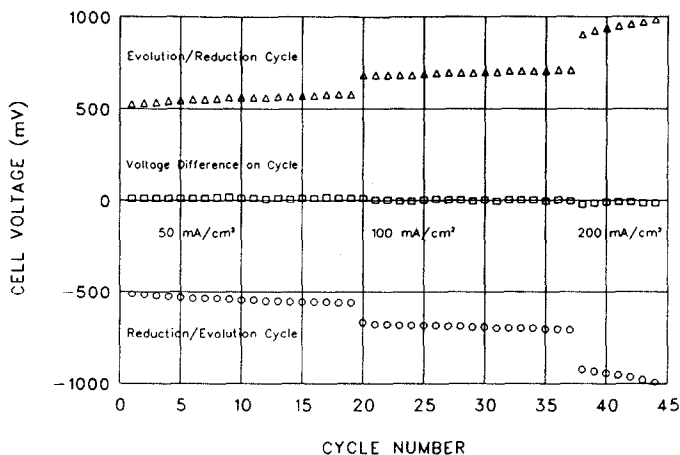


Fig. 2.  $\text{O}_2/\text{O}_2$  cell cycling test of  $\text{Na}_x\text{Pt}_3\text{O}_4$ : 30 min  $\text{O}_2$  reduction/evolution, 5 min open circuit, 30 min evolution/reduction, 30% KOH,  $80^\circ\text{C}$ , 50 psi  $\text{O}_2$ .

515–575 mV at 50 mA/cm<sup>2</sup>; 670–710 mV at 100 mA/cm<sup>2</sup>; and 900–995 mV at 200 mA/cm<sup>2</sup>. The total cell potential increased slightly over time at 50 and 100 mA/cm<sup>2</sup>. The cell potential increased more rapidly over time at 200 mA/cm<sup>2</sup>. The difference between the absolute values of cell voltage on positive and negative portions of the cycle was near zero, indicating that the two electrodes were performing nearly identically, as expected.

This material is one of the best candidate bifunctional oxygen electrode catalysts developed to date in terms of both stability and oxygen reduction/evolution performance. The emphasis in the current development effort is on preparing larger quantities of single-phase material and correlating synthesis conditions, crystalline structure, sodium deficiency and performance. A number of our earlier attempts, for reasons we have not clearly established, contained a second phase of free Pt, probably from partial decomposition of the PtO<sub>2</sub> reactant. Generally this two-phase material exhibited lower conductivity and surface area and poorer performance than single-phase Na<sub>x</sub>Pt<sub>3</sub>O<sub>4</sub>. The Pt phase can be partially dissolved out with hot aqua regia, which improves conductivity, surface area and performance, but not significantly. Several recent preparations have yielded single-phase, conductive material, but the performance is lower than observed earlier. At the present time, we are trying to determine Na/Pt ratios by elemental analysis (ICP) for greater accuracy than that obtained from typical XRD back-reflection data. Some oxygen electrode performance data for recent preparations of Na<sub>x</sub>Pt<sub>3</sub>O<sub>4</sub>, compared to data presented in earlier publications, is shown in Fig. 3.

#### *Rh-RhO<sub>2</sub>, Pt-IrO<sub>2</sub>, Pt-RhO<sub>2</sub>*

Three noble-metal/noble-metal-oxide electrodes were prepared: Rh–RhO<sub>2</sub>, Pt–IrO<sub>2</sub> and Pt–RhO<sub>2</sub>. The fabrication methods used to make these electrodes were chosen as our best estimate of a balanced mix of hydrophobic/hydrophilic character. Oxygen reduction performance often benefits from a more hy-

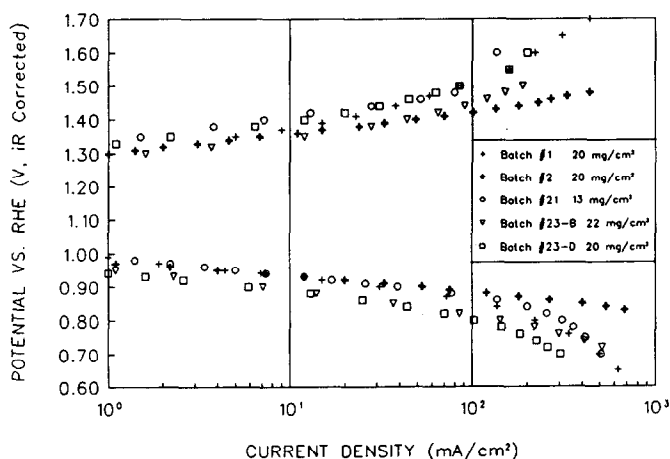


Fig. 3. O<sub>2</sub> reduction/evolution performance of Na<sub>x</sub>Pt<sub>3</sub>O<sub>4</sub>, 30% KOH, 80 °C.

dophobic electrode character while a hydrophilic electrode may be better for oxygen evolution. Giner, Inc. has developed a unique proprietary process for controlling the hydrophilic/hydrophobic properties at the particle level and applied this technology for achieving superior bifunctional oxygen electrode performance.

The oxygen electrode performance of these three mixed-character electrodes was tested in evolution and reduction modes, as discussed below. In each case, earlier data on the performance of the individual component materials (Pt, Rh,  $\text{RhO}_2$  and  $\text{IrO}_2$ ) as oxygen electrodes is compared to the performance of the mixed electrode structure. (The single-catalyst electrodes were also single-character structures, which usually compromises the performance in both modes.) In addition, the performance of the three mixed-character electrodes are compared directly.

In Fig. 4, the oxygen electrode performance of Rh black,  $\text{RhO}_2$  and Rh/ $\text{RhO}_2$  are compared versus the standard baseline materials: Pt for  $\text{O}_2$  evolution and 10% Pt/Au for  $\text{O}_2$  reduction. The Rh black,  $\text{RhO}_2$  and Rh/ $\text{RhO}_2$  electrodes all showed very similar  $\text{O}_2$  evolution performance, achieving  $200 \text{ mA/cm}^2$  at about 1.43 V versus RHE. The Rh black and Rh/ $\text{RhO}_2$  electrodes also showed very similar  $\text{O}_2$  reduction performance,  $200 \text{ mA/cm}^2$  at about 0.8 V; the  $\text{RhO}_2$  alone did not perform as well. The level of improvement in  $\text{O}_2$  reduction performance of the Rh/ $\text{RhO}_2$  electrode over that of the  $\text{RhO}_2$  electrode, was about 50 mV at  $200 \text{ mA/cm}^2$ . The mixed character of the Rh/ $\text{RhO}_2$  electrode is believed to be the reason for the performance improvement.

The first mixed-character Pt/ $\text{RhO}_2$  electrode (A) showed little improvement over the  $\text{RhO}_2$  electrode, as shown in Fig. 5. The performance of the two electrodes in both evolution and reduction modes is very similar,  $200 \text{ mA/cm}^2$  at about 0.77–0.78 V in  $\text{O}_2$  reduction and at about 1.42–1.43 V in

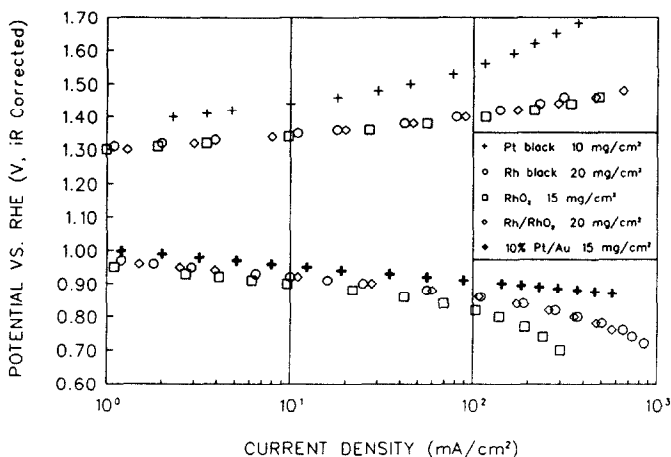


Fig. 4.  $\text{O}_2$  reduction/evolution performance of Rh,  $\text{RhO}_2$  and Rh/ $\text{RhO}_2$  electrodes, 30% KOH,  $80^\circ\text{C}$ .

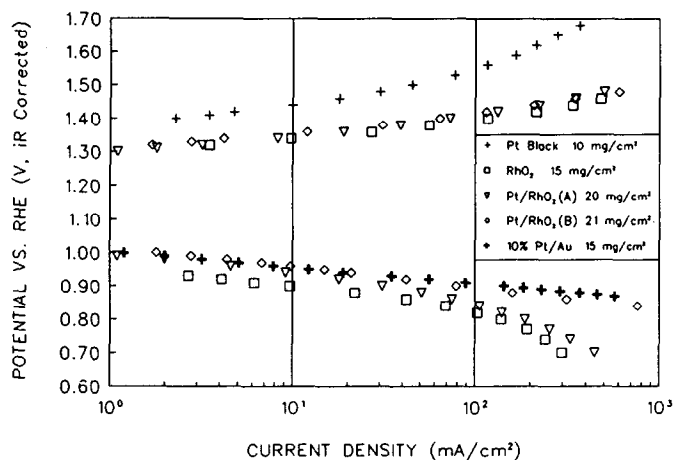


Fig. 5. O<sub>2</sub> reduction/evolution performance of RhO<sub>2</sub> and Pt/RhO<sub>2</sub> electrodes, 30% KOH, 80 °C.

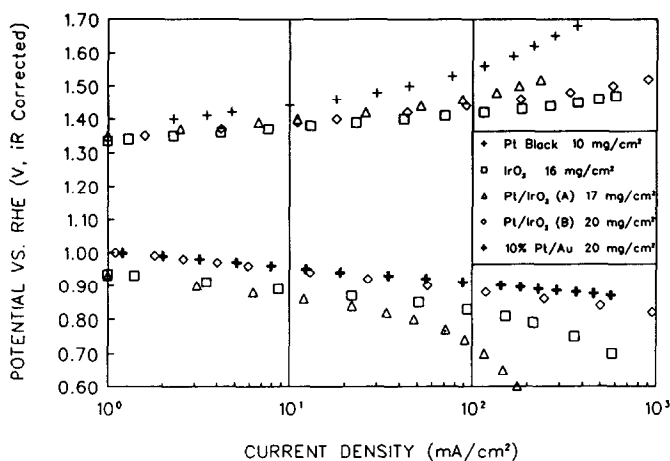


Fig. 6. O<sub>2</sub> reduction/evolution performance of IrO<sub>2</sub> and Pt/IrO<sub>2</sub> electrodes, 30% KOH, 80 °C.

O<sub>2</sub> evolution. Post-test examination of the electrode suggested that the hydrophobic/hydrophilic character was not balanced in this trial (too wettable). Therefore, a second Pt/RhO<sub>2</sub> electrode (B) was fabricated using a slightly different mixture ratio. As shown in Fig. 5, the resulting improvement in O<sub>2</sub> reduction performance was dramatic. The electrode was almost as good as the baseline 10% Pt/Au material. The O<sub>2</sub> evolution performance was basically unchanged.

In Fig. 6, pure Pt black and pure IrO<sub>2</sub> electrodes are compared to Pt/IrO<sub>2</sub> electrodes prepared by two different approaches. The catalyst for electrode A was prepared in an Adams co-fusion of Pt and Ir chlorides and was fabricated as a single-character electrode. The mixed-character Pt/IrO<sub>2</sub> elec-

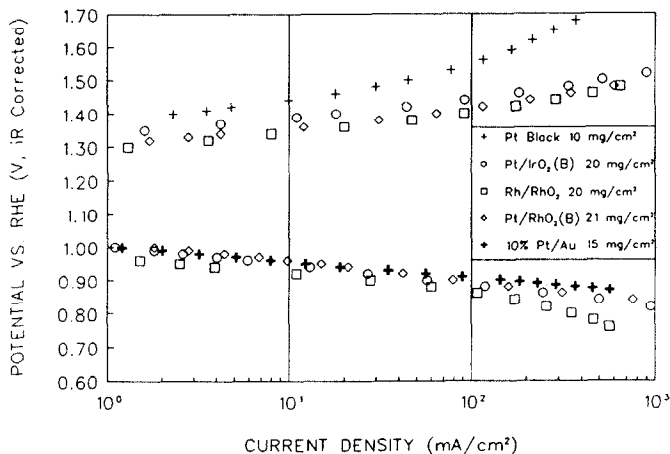


Fig. 7.  $O_2$  reduction/evolution performance of 'dual-character' bifunctional electrodes, 30% KOH, 80 °C.

trode (B) showed excellent  $O_2$  reduction performance, greatly improved over that of pure  $IrO_2$  or the co-fusion single-character Pt/ $IrO_2$  electrode. This optimized electrode sustained  $200 \text{ mA/cm}^2$  at about 0.87 V. This level of performance is close to that of the baseline catalyst, 10% Pt/Au, which held about 0.89 V at  $200 \text{ mA/cm}^2$ . In  $O_2$  evolution, the mixed-character Pt/ $IrO_2$  electrode also showed good performance,  $200 \text{ mA/cm}^2$  at about 1.47 V. This level of performance was slightly lower than that for  $IrO_2$ , but was better than the co-fusion single-character Pt/ $IrO_2$  electrode.

The performance of the three mixed-character electrodes is shown in Fig. 7. In  $O_2$  reduction mode, the Pt/ $RhO_2$  and Pt/ $IrO_2$  electrodes are very similar in performance and very close to the 10% Pt/Au baseline electrode. In  $O_2$  evolution mode, all three electrodes show similar superior performance; the Pt/ $RhO_2$  and Rh/ $RhO_2$  electrodes showed slightly better performance than the Pt/ $IrO_2$  electrode.

## Conclusions

Two materials of lower catalytic activity that have been identified as potential bifunctional alkaline oxygen electrode supports are  $LiNiO_x$  and ZrN. Two other materials, TiN and ZrC, do not appear to be sufficiently stable at oxidation potentials, but ZrC may be suitable as a catalyst support for oxygen reduction. Of the more catalytic candidate supports,  $LaNiO_3$  and  $PbPdO_2$  appear to be stable but need surface area development;  $CoIrO_3$  and  $NiIrO_3$  have been prepared in high-surface-area forms and show some oxygen evolution activity but need stability testing;  $RhO_2$  and  $IrO_2$  have been prepared in very high-surface-area forms, they appear to be stable and show high activity for oxygen evolution.



Recent work has focused on more complete development of the most promising bifunctional oxygen electrode catalyst,  $\text{Na}_x\text{Pt}_3\text{O}_4$ , and the application of wettability control at the catalyst/Teflon particle level to achieve superior bifunctional electrode operation. The latter approach has been successfully implemented with two catalysts integrated into 'dual-character' electrodes, e.g. Pt/IrO<sub>2</sub>, Pt/RhO<sub>2</sub> or Rh/RhO<sub>2</sub>. The same approach can be applied to a single bifunctional catalyst also, e.g. a 'dual-character'  $\text{Na}_x\text{Pt}_3\text{O}_4$  electrode. Such electrodes show highly efficient bifunctional oxygen electrocatalysis.

## Acknowledgements

This work was supported by NASA Lewis Research Center under the direction of Dr William Fielder and Dr Richard Baldwin, Contract No. NAS3-24635. We would like to acknowledge the assistance of Professor B. L. Chamberland of the University of Connecticut in the selection and identification of numerous materials tested in this program.

## References

- 1 L. Swette and J. Giner, *J. Power Sources*, 22 (1988) 399–408.
- 2 L. Swette and N. Kackley, Rechargeable alkaline oxygen electrode development, *Proc. American Institute of Chemical Engineers Annual Meet., San Francisco, CA, Nov. 5–10, 1989*.
- 3 L. Swette and N. Kackley, *J. Power Sources*, 29 (1990) 423–436.
- 4 J. Giner and S. Smith, *Electrochem. Technol.*, 5 (1967) 59–61.
- 5 R. Adams and R. L. Shriner, *J. Am. Chem. Soc.*, 45 (1923) 2171–2179.
- 6 K. B. Schwartz, C. T. Prewitt, R. D. Shannon, L. M. Corliss, J. M. Hastings and B. L. Chamberland, *Acta Crystallogr.*, 38 (1982) 363–368.
- 7 R. D. Shannon, T. E. Gier, P. F. Carcia, P. E. Bierstedt, R. B. Flippen and A. J. Vega, *Inorg. Chem.*, 21 (1982) 3372–3381.
- 8 B. L. Chamberland and S. Silverman, *J. Less Common Met.*, 65 (1979) 41–48.
- 9 M. E. Mullins and E. Riley, *J. Mater. Res.*, 4 (1989) 408–411.
- 10 H. S. Horowitz, J. M. Longo and J. T. Lewandowski, *Inorganic Synthesis*, Vol. 22, Wiley, New York, 1983, pp. 69–72.